

Quantum Quenches in a XXZ Spin Chain from a Spatially Inhomogeneous Initial State

Jarrett Lancaster¹ and Aditi Mitra¹

¹*New York University, Department of Physics, 4 Washington Place, New York, NY 10003*

(Dated: April 12, 2019)

Results are presented for the nonequilibrium dynamics of a quantum XXZ -spin chain whose spins are initially arranged in a domain wall profile via the application of a magnetic field in the z -direction which is spatially varying along the chain. The system is driven out of equilibrium in two ways: a). by rapidly turning off the magnetic field, b). by rapidly quenching the interactions at the same time as the magnetic field is turned off. The time-evolution of the domain wall profile as well as various two-point spin correlation functions is studied by the exact solution of the fermionic problem for the XX chain and via a bosonization approach and a mean-field approach for the XXZ chain. At long times the magnetization is found to equilibrate, while the two-point correlation functions in general do not. In particular, for quenches within the gapless XX phase, the transverse spin correlation functions acquire a spatially inhomogeneous structure at long times whose details depend on the initial domain wall profile. The spatial inhomogeneity is also recovered for the case of classical spins initially arranged in a domain wall profile and shows that the inhomogeneities arise due to the dephasing of transverse spin components as the domain wall broadens. A generalized Gibb's ensemble approach is found to be inadequate in capturing this spatially inhomogeneous state.

PACS numbers: 71.10.Pm, 02.30.Ik, 37.10.Jk, 05.70.Ln

I. INTRODUCTION

Recent years have seen remarkable progress in manipulating cold-atom systems¹ providing us with almost ideal realizations of strongly correlated many-particle systems. Cold atom systems also have the unique feature that the interactions between particles and the external potentials that they are subjected to are highly tunable and can be changed rapidly in time, thus driving these systems into highly nonequilibrium states². This property has in turn motivated a lot of theoretical activity that revolves around studying nonequilibrium time-evolution of strongly correlated systems arising due to a sudden change in some parameter of the Hamiltonian referred to as a “quantum quench”. The general consensus is that if the strongly correlated system is integrable, their time-evolution from some arbitrary initial state is highly constrained by the initial conditions so that these systems do not equilibrate but instead reach interesting nonequilibrium time-dependent or time-independent steady states.

In this paper we study quenched dynamics in one such integrable model, namely the XXZ spin chain. This model shows rich behavior even in its ground state³. For example, it exhibits a quantum critical point at $J_z = \pm J$ where J is the exchange interactions for the x, y components of the spins, and J_z is the exchange interaction for the z component of the spins. For $|J/J_z| > 1$, the ground state is an XX phase characterized by a gapless single particle spectrum, while for $|J/J_z| < 1$, the spins are in an Ising phase where the excitation spectrum is gapped.

Nonequilibrium dynamics of the XXZ model arising due to quenches has been a very active area of research (see for example^{4,5}). While most previous work has studied quenched dynamics in spatially homogeneous systems, in this work we consider the nonequilibrium time-

evolution arising from quenching from an initial state which is spatially inhomogeneous. Such an initial state is created by the application of an external magnetic field in the z direction that varies in magnitude along the chain, changing its sign at some point so that the spins are aligned in a domain wall pattern. (See⁶ for an experimental realization of such a setup). We study nonequilibrium dynamics that arise in the following two ways: a). by a sudden quench of the magnetic field to zero; b). by a sudden quench of the magnetic field to zero along with a quench in the magnitude of the exchange interactions. Thus we are always interested in a situation where the time evolution is due to a final Hamiltonian that has a spatially homogeneous ground state. We would like to understand how the system evolves in time after the quench, and whether the initial inhomogeneity affects the properties of the system at long times.

We study both single-particle expectation values corresponding to the local magnetization and two particle expectation values related to various spin-spin correlation functions. We find that the magnetization always equilibrates, however the details of how the domain wall profile evolves in time depends on whether the system after the quench is in the gapless XX phase or the gapped Ising phase^{7,8}. For example in the gapless phase the domain wall is found to spread out ballistically, however in the gapped phase the dynamics is much more complicated showing oscillations and revivals at short time scales. On the other hand, two-particle expectation values in particular those related to the transverse spin-correlation function show a lack of equilibration reaching a nonequilibrium steady state that is also found to be spatially inhomogeneous. The length scale of the spatial inhomogeneity depends on the details of the initial domain wall profile and is found to arise due to the dephasing of the

transverse spin components as the domain wall broadens.

The paper is organized as follows. In section II we study a XX chain which is initially subjected to a spatially varying magnetic field so that the spins are arranged in a domain wall profile. We study the nonequilibrium dynamics that arises when this magnetic-field is suddenly switched off. These results are obtained from the exact solution of a fermionic problem where an external magnetic field that varies linearly in position is equivalent to an effective electric field on the fermions. In section III the effect of quenching only a spatially varying magnetic field in a XXZ chain is studied via a bosonization approach. The results of section II and III are found to be in qualitative agreement and in particular recover ballistic domain wall motion and spatial inhomogeneities in the transverse spin correlation function. A physical explanation for this inhomogeneity is provided in section IV where the problem of quenching a spatially varying magnetic field is studied classically and a spin-wave pattern is obtained as a long time solution of a Landau-Lifshitz equation.

In section V, the effect of simultaneously quenching the magnetic field and interactions is studied using a bosonization approach. In section V A results are presented for the case when the quench is entirely within the gapless XX phase. The spatial inhomogeneities in the correlation functions are recovered along with the nonequilibrium exponents obtained earlier in a purely homogeneous quench^{9,10}. In section V B the effect of quenching into the gapped Ising phase is studied via a semiclassical approach. Here we find the domain wall dynamics to be qualitatively different, however at long times we find that all inhomogeneities eventually decay away. The latter result may very well be an artifact of the semiclassical approach which neglects creation of solitons. The results of the bosonization approach is complemented by a mean-field treatment in section VI. Finally we conclude in section VII.

II. QUENCH OF A SPATIALLY VARYING MAGNETIC FIELD IN A XX CHAIN: EXACT SOLUTION OF THE FERMIONIC PROBLEM

In this section we will study an XX chain in a magnetic field in the z direction that varies linearly in position, and changes sign at $x = 0$, so that the ground state is a domain wall configuration. In subsection II A we will study the properties of this domain wall state, and in subsequent subsections study the nonequilibrium time-evolution arising when the the spatially varying magnetic field is suddenly switched off.

A. Creation of domain-wall state

Our starting point is the XX Hamiltonian,

$$H_{xx} = -J \sum_j \left[S_j^x S_{j+1}^x + S_j^y S_{j+1}^y - \frac{h_j}{J} S_j^z \right], \quad (1)$$

where $S_j^\nu = \frac{1}{2} \sigma_j^\nu$, σ^ν are Pauli matrices, h_j is an external magnetic field aligned along the \hat{z} direction, and J is the exchange energy. For a uniform magnetic field, the Hamiltonian may be diagonalized by a Jordan-Wigner transformation.¹¹⁻¹⁴ An overview of this calculation can be found in Appendix A.

To create an inhomogeneous state we will consider a linearly varying field $h_j = \mathcal{F}ja$, where a is a lattice spacing. After the Jordan-Wigner transformation the system maps to the Wannier-Stark problem^{15,16} of electrons in a lattice subjected to a constant force (or electric field) \mathcal{F} ,

$$H_{xx} = -\frac{J}{2} \sum_j \left[c_j^\dagger c_{j+1} + c_{j+1}^\dagger c_j \right] + \sum_j j \mathcal{F} a c_j^\dagger c_j \quad (2)$$

The Hamiltonian can be diagonalized

$$H_{xx} = \sum_m \epsilon_m \eta_m^\dagger \eta_m, \quad (3)$$

with

$$\epsilon_m = m \mathcal{F} a, \quad (\forall m = \text{integer}), \quad (4)$$

and

$$\begin{aligned} \eta_m^\dagger &= \sum_j J_{j-m} \left(\frac{J}{\mathcal{F}a} \right) c_j^\dagger \\ &= \frac{1}{\sqrt{N}} \sum_k \exp \left[-ikma - i \frac{J}{\mathcal{F}a} \sin(ka) \right] c_k^\dagger \end{aligned} \quad (5)$$

where $c_j = \frac{1}{\sqrt{N}} \sum_k c_k e^{ikj}$, N is the total number of sites and $J_n(x)$ is a Bessel function of the first kind. We construct the ground state $|\Psi\rangle$ by including all negative energy states,

$$|\Psi\rangle = \prod_{m<0} \eta_m^\dagger |0\rangle. \quad (7)$$

This is a domain-wall state with a characteristic width $\frac{x}{a} \equiv \alpha = \frac{J}{\mathcal{F}a}$ to the left (right) of which all spins are up (down). This can be seen by evaluating the magnetization at the position ja

$$m^z(j) = \langle \Psi | c_j^\dagger c_j | \Psi \rangle - \frac{1}{2}. \quad (8)$$

which on rewriting c_j, c_j^\dagger in terms of the diagonal η_m operators is found to be

$$m^z(j) = -\frac{1}{2} + \sum_{m \geq 0} J_{j+m}^2(\alpha) \quad (9)$$

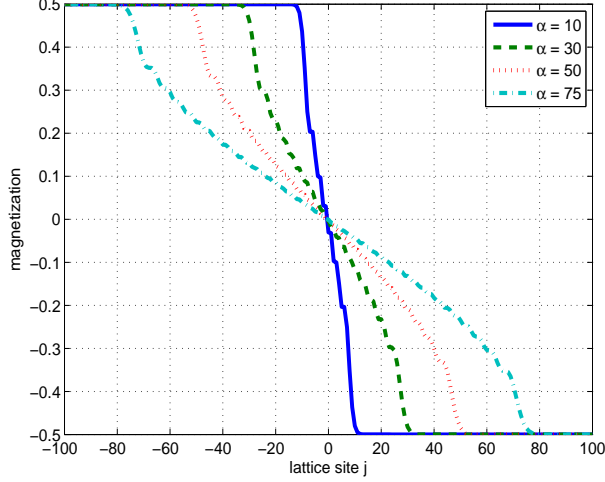


FIG. 1: Plot of the initial magnetization for various values of $\alpha = \frac{J}{\mathcal{F}a}$.

Upon noting that the support of $J_n(x)$ is only for $x \sim n^{17}$, and recalling the identity¹⁸ $\sum_n J_n^2(x) = 1$, it is easy to see that this indeed describes the claimed domain-wall state. Eq. 9 is also plotted in Fig. 1. It is worth noting that the case of $\alpha = 0$ corresponds to an infinite “electric field” \mathcal{F} that forces a sharp wall of zero width. This case was investigated by Antal *et al*¹⁹. We will extend some of their results to more general domain walls, and also study two-particle correlation functions.

The basic spin correlation functions that we will compute are,

$$C^{\nu\nu}(j, j+n) = \langle S_j^\nu S_{j+n}^\nu \rangle, \quad (\nu = x, z) \quad (10)$$

These may be expressed in terms of Majorana operators¹¹ $A_j = c_j^\dagger + c_j$, and $B_j = c_j^\dagger - c_j$ as follows,

$$C^{zz}(j, j+n) = \frac{1}{4} \langle B_j A_j B_{j+n} A_{j+n} \rangle, \quad (11)$$

and

$$C^{xx}(j, j+n) = \frac{1}{4} \langle B_j A_{j+1} B_{j+1} \cdots A_{j+n-1} B_{j+n-1} A_{j+n} \rangle, \quad (12)$$

The above correlations can be evaluated by rewriting c_i in terms of η_m and applying Wick’s theorem. The basic contractions are²⁰

$$\begin{aligned} \langle B_j A_{j+n} \rangle &= -\langle A_j B_{j+n} \rangle = \sum_{m>0} [J_{j+m}(\alpha) J_{j+n+m}(\alpha) \\ &\quad - J_{j-m}(\alpha) J_{j+n-m}(\alpha)], \end{aligned} \quad (13)$$

$$\langle A_j A_{j+n} \rangle = -\langle B_j B_{j+n} \rangle = \delta_{n=0}. \quad (14)$$

Using some Bessel function identities, the mixed contraction can be simplified to

$$\begin{aligned} \langle B_j A_{j+n} \rangle &= \frac{\alpha}{2n} [J_{j+n}(\alpha) J_{j+1}(\alpha) - J_{j+n+1}(\alpha) J_j(\alpha) \\ &\quad - J_{j+n}(\alpha) J_{j-1}(\alpha) + J_{j+n-1}(\alpha) J_j(\alpha)]. \end{aligned} \quad (15)$$

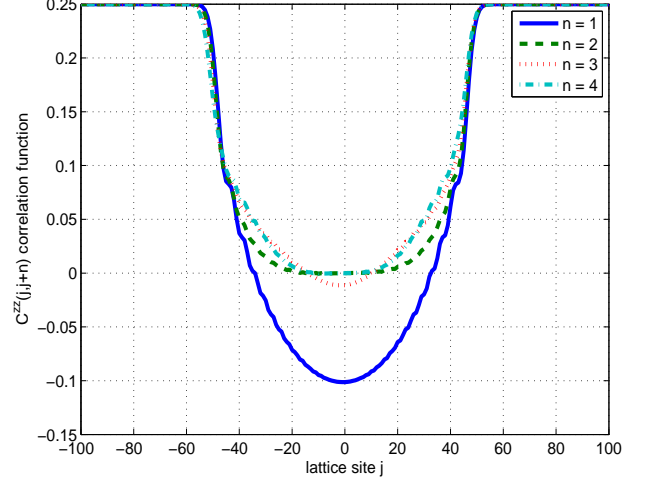


FIG. 2: Plot of $C^{zz}(j, j+n)$ for $n = 1, 2, 3, 4$ and $\alpha = \frac{J}{\mathcal{F}a} = 50$.

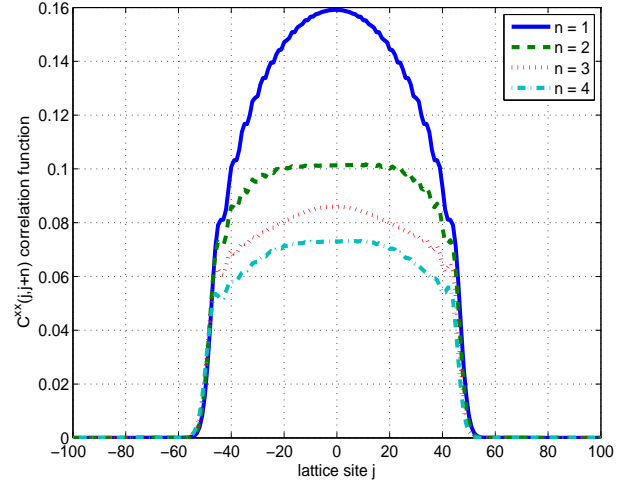


FIG. 3: Plot of $C^{xx}(j, j+n)$ for $n = 1, 2, 3, 4$ and $\alpha = \frac{J}{\mathcal{F}a} = 50$.

Since we encounter no contractions of the form $\langle A_i A_i \rangle$, the function $C^{xx}(j, j+n)$ may be written¹¹ as a Toeplitz determinant which is a computationally cheap task. In the next sub-section when we evaluate the correlation functions after a quench of the magnetic field, we will find $\langle A_j A_{j+n} \rangle \neq 0$ in the nonequilibrium state. In this case, the evaluation of C^{xx} will require computing the square root of a Pfaffian¹³.

The correlation functions C^{zz} and C^{xx} for $\alpha = 50$ are given in Fig. 2 and Fig. 3 respectively.

B. Domain wall dynamics after the magnetic field quench

We will now explore the dynamics that arises when the spatially varying magnetic field is suddenly switched off at $t = 0$ i.e., $h_j(t) = \theta(-t)\mathcal{F}ja$. Thus at $t < 0$ the many-body wavefunction of the system is Eq. 7, while for $t > 0$, as shown in Appendix A, the wave-function evolves according to the Hamiltonian,

$$H_f = \sum_k \epsilon_k c_k^\dagger c_k \quad (16)$$

where $\epsilon_k = -J \cos(ka)$.

The time-dependent magnetization is given by

$$m^z(j, t) = \langle \Psi | c_j^\dagger(t) c_j(t) | \Psi \rangle - \frac{1}{2}. \quad (17)$$

The time-evolution of c_j, c_j^\dagger in terms of the η_m operators is given in Eqns. A6, A7 from which we obtain

$$m^z(j, t) = -\frac{1}{2} + \sum_{m>0} |L(j+m, t, \alpha)|^2, \quad (18)$$

where

$$L(j+m, t, \alpha) = \int_{-\pi}^{\pi} \frac{dk}{2\pi} e^{ik(j+m) - i\epsilon_k t - i\alpha \sin k}. \quad (19)$$

Evaluating the integral, we find

$$m^z(j, t) = -\frac{1}{2} + \sum_{m>0} J_{j+m}^2 \left(\sqrt{(Jt)^2 + \alpha^2} \right). \quad (20)$$

This corresponds to a wall whose width $W = Jat$ increases linearly and hence ballistically in time with a velocity of Ja . Setting $\alpha = 0$, we recover the result of Antal *et al*¹⁹.

C. Correlation functions after the magnetic field quench

We now turn to the evaluation of the longitudinal and transverse correlation functions given in Eqns. (11) and (12) at a time t after the quench. The basic contractions that we need are $\langle B_j(t)A_{j+n}(t) \rangle$ and $\langle A_j(t)A_{j+n}(t) \rangle$ for which we find the following expressions

$$\begin{aligned} \langle B_j(t)A_{j+n}(t) \rangle = & \\ \frac{r}{2n} [e^{in\delta} (J_{j+n}(r)J_{j+1}(r) - J_{j+n+1}(r)J_j(r)) & \\ - e^{-in\delta} (J_{j+n}(r)J_{j-1}(r) - J_{j+n-1}(r)J_j(r))] , & (21) \end{aligned}$$

$$\begin{aligned} \langle A_j(t)A_{j+n}(t) \rangle = & \\ \frac{r}{2n} [e^{in\delta} (J_{j+n}(r)J_{j+1}(r) - J_{j+n+1}(r)J_j(r)) & \\ + e^{-in\delta} (J_{j+n}(r)J_{j-1}(r) - J_{j+n-1}(r)J_j(r))] , & (22) \end{aligned}$$

with $r = \sqrt{(Jt)^2 + \alpha^2}$ and $\tan \delta \equiv Jt/\alpha$. As before, we have $\langle B_j(t)B_{j+n}(t) \rangle = -\langle A_j(t)A_{j+n}(t) \rangle$ and $\langle B_j(t)A_{j+n}(t) \rangle = -\langle A_j(t)B_{j+n}(t) \rangle$.

The transverse correlation function $C^{xx}(j, j+n, t)$ is given by

$$|C^{xx}(j, j+n, t)| = \frac{1}{4} \sqrt{\det \mathbf{C}}, \quad (23)$$

where \mathbf{C} is the anti-symmetric matrix

$$\mathbf{C} = \begin{pmatrix} \mathbf{S} & \mathbf{G} \\ -\mathbf{G} & \mathbf{Q} \end{pmatrix}, \quad (24)$$

with the $n \times n$ sub-matrices defined by

$$S_{ik} = -S_{ki} = \langle B_{i+j-1} B_{k+j-1} \rangle \quad (k > i) \quad (25)$$

$$Q_{ik} = -Q_{ki} = \langle A_{i+j} A_{k+j} \rangle \quad (k > i) \quad (26)$$

$$G_{ik} = \langle B_{i+j-1} A_{k+j} \rangle. \quad (27)$$

Note that both \mathbf{S} and \mathbf{Q} are anti-symmetric, and thus defined by the elements with $k > i$, while no such restriction is placed on \mathbf{G} .

The numerical evaluation of the above expression for $\alpha = 25$ is shown in Fig. 4 for three different times: $t = 0$, an intermediate time and for long times where one finds the appearance of a spatially oscillating pattern.

In order to get some insight into the long time behavior of the system, we consider the limit of $r \rightarrow \infty$ while imposing the condition $j, j+n \ll r$ on the two position indices of the correlation functions. This limit corresponds to a very broad domain wall which may arise either due to a very weak electric field $\alpha \gg 1$ at arbitrary times t (and hence arbitrary δ) or could arise on waiting long enough after a quench so that an initial narrow domain wall has had enough time to broaden. The condition on the position indices imply that we are looking at correlations in the vicinity of the center of the domain wall where the magnetization has locally equilibrated. Using the asymptotic expansion for the Bessel functions with large arguments¹⁸, we find

$$\langle B_j(t)A_{j+n}(t) \rangle \sim \frac{2 \cos(n\delta)}{\pi n} \sin\left(\frac{n\pi}{2}\right), \quad (28)$$

$$\langle A_j(t)A_{j+n}(t) \rangle \sim \frac{2i \sin(n\delta)}{\pi n} \sin\left(\frac{n\pi}{2}\right) \quad (29)$$

Substituting the asymptotic expansions in Eq. 28, Eq. 29 we find,

$$C^{zz}(j, j+n, t) \longrightarrow C_{eq}^{zz}(n) = -\frac{\sin^2\left(\frac{\pi n}{2}\right)}{\pi^2 n^2} \quad (30)$$

where $C_{eq}^{ab}(n)$ is the equilibrium result (i.e. the result in the ground state of H_f) for the ab correlation function¹⁴.

Employing the asymptotic expansions in the evaluation of $C^{xx}(j, j+n)$, we have verified through $n \sim 1000$ that

$$C^{xx}(j, j+n, t) = C_{eq}^{xx}(n) \cos(n\delta) \quad (31)$$

$$\xrightarrow{t \rightarrow \infty} C_{eq}^{xx}(n) \cos\left(\frac{\pi n}{2}\right) \quad (32)$$

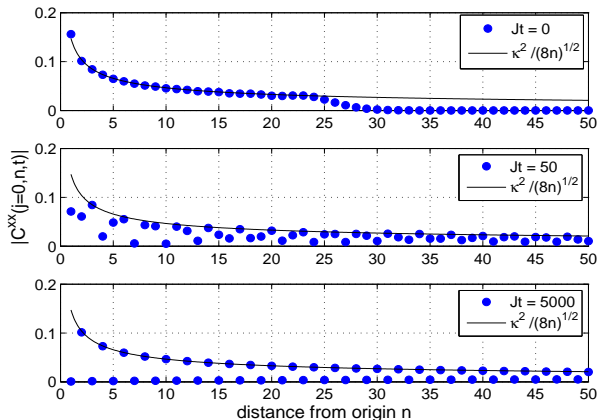


FIG. 4: Time evolution of $C^{xx}(j=0, n)$ correlation function for $\alpha = 25$. Solid line is the equilibrium correlation function C_{eq}^{xx} .

where $C_{eq}^{xx}(n)$ is the equilibrium value of the xx -correlation function¹¹ which has the asymptotic form²¹,

$$C_{eq}^{xx}(n) \approx \frac{1}{\sqrt{8n}} \kappa^2, \quad (33)$$

with $\log \kappa = \frac{1}{4} \int_0^\infty \frac{dt}{t} (e^{-4t} - \frac{1}{\cosh^2 t})$.

Thus the main results of this section on the effect of quenching a spatially varying magnetic field in a XX model are as follows: a). An initial domain wall spreads out ballistically after the magnetic field quench so that the magnetization equilibrates to its homogeneous ground state value of $m^z = 0$. For a sharp domain wall, ($\alpha = \frac{J}{F_a} \ll 1$), the magnetization at a distance na from the center of the domain wall begins to equilibrate after a time $Jt \sim na$. This is an example of the horizon effect^{22,23}, namely the minimal time required for ballistically propagating excitations from the center of the domain wall to reach the observed point; b). Another consequence of the horizon effect is that any two point correlation function $C^{ab}(j, j+n)$ is found to change significantly only after times $Jt > \min(|j|, |j+n|)$ ²³ for $\alpha \ll 1$; c). While the $C^{zz}(j, j+n)$ correlation function eventually equilibrates at long times, the $C^{xx}(j, j+n)$ correlation function reaches a nonequilibrium steady state at times $\min(\sqrt{\alpha^2 + (Jt)^2}, tFa) \gg 1$ to a value given by Eq. 32 which is basically the equilibrium correlation function with oscillations at a wave-vector $\mathcal{O}(k_F = \frac{\pi}{2a})$ superimposed on it.

Note that the effect of quenching from an initial domain wall state was studied in²⁴ using the methods of boundary conformal field theory. Detailed results were presented for the case where the time-evolution is due to the Ising model ($J \sum_i S_i^x S_{i+1}^x + h \sum_i S_i^z$), and were then extended to the general case. Our results differ from those of²⁴ for the general spin chain in two important ways. One is that at long times we recover a spatial

spin-wave pattern that was not captured in²⁴. Secondly at long times after the quench, our two-point correlation functions continue to be critical (i.e., have a power-law decay) whereas the results of²⁴ point to thermal behavior with exponential decay in the two-point correlation function. The differences may be due to the particular choice of boundary conditions used in²⁴.

In subsequent sections we will study the effect of quenching a spatially varying magnetic field with and without an interaction quench in a XXZ chain using a bosonization approach. For quenches within the gapless XX phase, results of this section, namely critical behavior in the two-point correlation function even after the quench, and the presence of spatial inhomogeneities will be recovered.

III. QUENCH OF A SPATIALLY VARYING MAGNETIC FIELD IN A XXZ CHAIN: BOSONIZATION APPROACH

In this section we will study a general XXZ chain which is subjected to a time-dependent spatially varying magnetic field. The most convenient way to study this problem is via the bosonization approach. We first review some of the notation.

A. Equilibrium correlations

A general XXZ-spin chain Hamiltonian in a magnetic field is

$$H = \sum_j \left[J \left(\hat{S}_j^x \hat{S}_{j+1}^x + \hat{S}_j^y \hat{S}_{j+1}^y \right) + J_z \hat{S}_j^z \hat{S}_{j+1}^z - h_j S_j^z \right], \quad (34)$$

The above can be mapped onto a Luttinger liquid with a back-scattering potential³,

$$H = \frac{u}{2\pi} \int dx \left[K(\nabla\theta)^2 + \frac{1}{K}(\nabla\phi)^2 \right] + \frac{1}{\pi} \int dx h(x) \nabla\phi - \frac{2g}{(2\pi\alpha)^2} \int dx \cos(2\phi(x)), \quad (35)$$

where $g = J_z a$, and the fields θ and ϕ are defined in terms of the boson creation/annihilation operators as

$$\phi(x) = -(N_R + N_L) \frac{\pi x}{L} - \frac{i\pi}{L} \sum_{p \neq 0} \left(\frac{L|p|}{2\pi} \right)^{1/2} \frac{1}{p} e^{-\alpha|p|/2 - ipx} (b_p^\dagger + b_{-p}), \quad (36)$$

$$\theta(x) = (N_R - N_L) \frac{\pi x}{L} + \frac{i\pi}{L} \sum_{p \neq 0} \left(\frac{L|p|}{2\pi} \right)^{1/2} \frac{1}{|p|} e^{-\alpha|p|/2 - ipx} (b_p^\dagger - b_{-p}) \quad (37)$$

where $N_{\sigma=R,L} = \sum_{p \neq 0} : \psi_\sigma^\dagger(p) \psi_\sigma(p) :$, and $:\dots:$ denotes normal ordering of operators. In the continuum

limit, we interpret $x = ja$ for some integer j and lattice spacing a . The coupling-parameter relationships are

$$uK = v_F = Ja \sin(k_F a), \quad (38)$$

$$\frac{u}{K} = v_F \left[1 + \frac{2J_z a}{\pi v_F} (1 - \cos(2k_F a)) \right]. \quad (39)$$

For an xy anti-ferromagnet ($J > 0$), the mapping from spin language to boson language is given by³

$$\hat{S}^z(x) = \frac{-1}{\pi} \nabla \phi(x) + \frac{(-1)^x}{\pi \alpha} \cos[2\phi(x)], \quad (40)$$

$$\hat{S}^+(x) = \frac{1}{\sqrt{2\pi\alpha}} \exp[-i\theta(x)] [(-1)^x + \cos[2\phi(x)]] \quad (41)$$

In equilibrium and zero magnetic fields, the magnetization and basic physical correlations in the gapless anti-ferromagnetic XX phase are

$$\langle \hat{S}^z(x) \rangle = -\frac{1}{\pi} \langle \nabla \phi(x) \rangle = 0, \quad (42)$$

$$\langle \hat{S}^z(x+n) \hat{S}^z(x) \rangle = C_1 \left(\frac{1}{n} \right)^2 + C_2 (-1)^n \left(\frac{1}{n} \right)^{2K} \quad (43)$$

$$\langle \hat{S}^+(x+n) \hat{S}^-(x) \rangle = C_3 \left(\frac{1}{n} \right)^{2K + \frac{1}{2K}} + C_4 (-1)^n \left(\frac{1}{n} \right)^{\frac{1}{2K}} \quad (44)$$

where the C_j are non-universal constants.

The antiferromagnetic Hamiltonian may be transformed to a ferromagnetic Hamiltonian by the transformation $S_j^\pm \rightarrow (-1)^j S_j^\pm$, resulting in ferromagnetic operators

$$\hat{S}^z(x)_{\text{f.m.}} = -\frac{1}{\pi} \nabla \phi(x) + \frac{(-1)^x}{\pi \alpha} \cos[2\phi(x)], \quad (45)$$

$$\hat{S}^+(x)_{\text{f.m.}} = \frac{1}{\sqrt{2\pi\alpha}} \exp[i\theta(x)] [1 + (-1)^x \cos[2\phi(x)]] \quad (46)$$

As a consequence, the magnetization and spin correlations in the gapless ferromagnetic XX phase are,

$$\langle \hat{S}^z(x) \rangle_{\text{f.m.}} = -\frac{1}{\pi} \langle \nabla \phi(x) \rangle = 0, \quad (47)$$

$$\langle \hat{S}^z(x+n) \hat{S}^z(x) \rangle_{\text{f.m.}} = C_1 \left(\frac{1}{n} \right)^2 + C_2 (-1)^n \left(\frac{1}{n} \right)^{2K} \quad (48)$$

$$\langle \hat{S}^+(x+n) \hat{S}^-(x) \rangle_{\text{f.m.}} = C_3 (-1)^n \left(\frac{1}{n} \right)^{2K + \frac{1}{2K}} + C_4 \left(\frac{1}{n} \right)^{\frac{1}{2K}}, \quad (49)$$

B. Magnetic field quench in the XX phase

1. Diagonalization

In this section we will study the time-dependent Hamiltonian

$$H = H_i \theta(-t) + H_f \theta(t) \quad (50)$$

We choose a point in the XX phase corresponding to $K = 1$ and $u = v_F$. Thus,

$$H_i = \frac{v_F}{2\pi} \int dx \left((\nabla \theta)^2 + (\nabla \phi)^2 + \frac{2}{v_F} h(x) \nabla \phi \right) \quad (51)$$

$$= \sum_{p \neq 0} v_F |p| a_p^\dagger a_p, \quad (52)$$

so that the initial state at $t \leq 0$ is the spatially inhomogeneous ground state of H_i . The magnetic field $h(x)$ is suddenly switched off at $t = 0$ so that the system evolves according to

$$H_f = \frac{v_F}{2\pi} \int dx ((\nabla \theta)^2 + (\nabla \phi)^2) \quad (53)$$

$$= \sum_{p \neq 0} v_F |p| b_p^\dagger b_p \quad (54)$$

Since Eq. 51 basically represents harmonic oscillators subjected to an electric field, it may be easily diagonalized by the shift,

$$b_p = a_p + \lambda_p. \quad (55)$$

where,

$$\lambda_p = \frac{1}{v_F \sqrt{2\pi|p|L}} h_p, \quad (56)$$

and h_p is the Fourier transform of $h(x)$. Taking $h(-x) = -h(x)$ (corresponding to a magnetic field that is anti-symmetric in space allowing for a domain wall solution), this gives

$$h_p = -i \int \sin(px) h(x) dx. \quad (57)$$

For some time t after the quench, it is straightforward to show that

$$\phi(x, t) = e^{iH_f t} \phi(x, 0) e^{-iH_f t} = \phi^a(x, t) + \delta\phi(x, t), \quad (58)$$

$$\theta(x, t) = e^{iH_f t} \theta(x, 0) e^{-iH_f t} = \theta^a(x, t) + \delta\theta(x, t), \quad (59)$$

where

$$\phi^a(x, t) = -\frac{i\pi}{L} \sum_{p \neq 0} \left(\frac{L|p|}{2\pi} \right)^{1/2} \times \frac{1}{p} e^{-\alpha|p|/2 - ipx} \left(a_p^\dagger e^{iv_F|p|t} + a_{-p} e^{-iv_F|p|t} \right), \quad (60)$$

$$\theta^a(x, t) = +\frac{i\pi}{L} \sum_{p \neq 0} \left(\frac{L|p|}{2\pi} \right)^{1/2} \times \frac{1}{|p|} e^{-\alpha|p|/2 - ipx} \left(a_p^\dagger e^{iv_F|p|t} - a_{-p} e^{-iv_F|p|t} \right). \quad (61)$$

Since we will be computing expectation values with respect to an initial state which is the ground state of the a_p operators, ϕ^a, θ^a will just return the equilibrium results. Thus the effects of the shift and hence the initial magnetic field is contained entirely in

$$\delta\phi(x, t) = \frac{i}{\pi v_F} \int_0^\infty \frac{dp}{p} \cos[pv_F t] \cos[px] h_p, \quad (62)$$

$$\delta\theta(x, t) = \frac{-i}{\pi v_F} \int_0^\infty \frac{dp}{p} \sin[pv_F t] \sin[px] h_p. \quad (63)$$

For any antisymmetric $h(x)$ the above reduces to,

$$\delta\phi(x, t) = \frac{1}{8v_F} \int_{-\infty}^\infty dx' h(x') [\text{sgn}[x' + z_-] + \text{sgn}[x' + z_+] + \text{sgn}[x' - z_+] + \text{sgn}[x' - z_-]], \quad (64)$$

$$\delta\theta(x, t) = \frac{1}{8v_F} \int_{-\infty}^\infty dx' h(x') [\text{sgn}[x' + z_+] - \text{sgn}[x' - z_+] - \text{sgn}[x' + z_-] - \text{sgn}[x' - z_-]], \quad (65)$$

where $\text{sgn}[x] \equiv x/|x|$, and $z_\pm = x \pm v_F t$.

The above implies that the magnetization before the quench is

$$\langle \hat{S}^z \rangle = -\frac{1}{\pi} \langle \frac{\partial\phi(x)}{\partial x} \rangle = -\frac{1}{\pi} \frac{\partial\delta\phi(x)}{\partial x} = \frac{1}{\pi v_F} h(x) \quad (66)$$

Thus within the bosonization approach, the magnetization follows the magnetic-field profile.

2. Magnetization and Correlations after the quench

The magnetization at some time t after the magnetic-field quench is

$$\begin{aligned} \langle \hat{S}^z \rangle &= -\frac{1}{\pi} \langle \partial_x \phi^a(x, t) \rangle - \frac{1}{\pi} \partial_x \delta\phi(x, t) \\ &= \frac{1}{2\pi v_F} (h(x + v_F t) + h(x - v_F t)) \end{aligned} \quad (67)$$

As anticipated, the domain wall spreads out with speed v_F in both directions. This result is consistent with the ballistic time-evolution found in section II from the exact solution of the fermionic problem.

Next we turn to the evaluation of the C^{xx} correlation function which for the fermionic model was found to be $\langle \hat{S}_{j+n}^x \hat{S}_j^x \rangle \rightarrow \cos\left(\frac{n\pi}{2}\right) C_{eq}^{xx}(n)$ where $C_{eq}^{xx}(n) \sim \frac{1}{\sqrt{n}}$ was the equilibrium correlation function. In the bosonization approach,

$$\langle \hat{S}^+(x+n) \hat{S}^-(x) \rangle \sim \exp[-i(\delta\theta(x+n, t) - \delta\theta(x, t))] \frac{1}{\sqrt{n}}. \quad (68)$$

Let us suppose

$$h(x) = h_0 \tanh(x/\xi) \quad (69)$$

implying

$$h_p = -ih_0 \left(\frac{\pi\xi}{\sinh\left(\frac{\pi p\xi}{2}\right)} \right) \quad (70)$$

Then we find,

$$\begin{aligned} \delta\theta(x+n, t) - \delta\theta(x, t) &= \\ &= -\frac{\xi h_0}{2v_F} \log \left[\frac{\cosh[(x - v_F t)/\xi] \cosh[(x+n + v_F t)/\xi]}{\cosh[(x+n - v_F t)/\xi] \cosh[(x + v_F t)/\xi]} \right] \\ &\xrightarrow{v_F t, |v_F t \pm x|, |v_F t \pm (x+n)| \gg \xi} -\frac{\xi h_0}{2v_F} \left[\frac{|x - v_F t|}{\xi} \right. \\ &\quad \left. + \frac{|x+n + v_F t|}{\xi} - \frac{|x+n - v_F t|}{\xi} - \frac{|x + v_F t|}{\xi} \right] \end{aligned} \quad (71)$$

For $v_F t \gg |x|, |x+n|$, i.e, long after the moving domain wall front has crossed the two observation points at x and $x+n$, we find

$$\delta\theta(x+n, t) - \delta\theta(x, t) \rightarrow \frac{h_0 n}{v_F}. \quad (72)$$

so that

$$\langle \hat{S}^+(x+n) \hat{S}^-(x) \rangle \sim e^{in h_0 / v_F} \left(\frac{1}{\sqrt{n}} \right). \quad (73)$$

Thus we find that the transverse correlation functions do not equilibrate but acquire a spatial oscillation at wave-vector h_0/v_F . This result is similar to that obtained from the exact solution of the fermionic problem. To make an exact correspondence between the two problems, note that for $t=0$ and $x \rightarrow \pm\infty$,

$$\langle S^z(x = \pm\infty) \rangle \rightarrow \pm \frac{h_0}{\pi v_F}, \quad (74)$$

whereas, in the fermionic problem, the magnetization approach $\mp \frac{1}{2}$ far from the wall. Thus the two problems map into each other when

$$\frac{h_0}{v_F} \rightarrow -\frac{\pi}{2a}, \quad (75)$$

so that writing $n = \bar{n}a$, where \bar{n} is an integer,

$$\langle S^+(x + \bar{n}a) S^-(x) \rangle \rightarrow e^{i\pi\bar{n}/2} \left(\frac{1}{\sqrt{\bar{n}}} \right), \quad (76)$$

giving us precisely the observed behavior of Eq. 32. In particular the wavelength of the oscillation is related to the change in the magnetization density from one end of the domain wall to the next, and is independent of the width of the domain wall ξ . The fermionic problem corresponded to the maximum possible change in magnetization, and hence the wavelength of the oscillation was found to be $\mathcal{O}(1/k_F)$.

For the evaluation of the $\langle S^z S^z \rangle$ correlation function, we need to evaluate $\exp[i\delta\phi(x+n, t) - i\delta\phi(x, t)]$. We find,

$$\delta\phi(x+n, t) - \delta\phi(x, t) = \frac{-h_0\xi}{2v_F} \log \left[\frac{\cosh \left[\frac{x+n+v_F t}{\xi} \right] \cosh \left[\frac{x+n-v_F t}{\xi} \right]}{\cosh \left[\frac{x+v_F t}{\xi} \right] \cosh \left[\frac{x-v_F t}{\xi} \right]} \right] \quad (77)$$

$\xrightarrow{v_F t \gg \xi, |x|, |x+n|} 0$

The above result together with the fact that

$$\begin{aligned} \partial_x \delta\phi(x+n, t) \partial_x \delta\phi(x, t) &= \\ \frac{1}{4\pi v_F^2} (h(x+v_F t) + h(x-v_F t)) & \\ \times (h(x+n+v_F t) + h(x+n-v_F t)). & \quad (78) \end{aligned}$$

implies that for $v_F t \gg \xi, |x|, |x+n|$, the C^{zz} correlation function equilibrates which is in agreement with the results in section II.

To summarize the results of this section: a). Within the bosonization approach, an applied magnetic-field produces a spin pattern that follows the local magnetic field. b). After a quench, the domain wall spreads out ballistically. The magnetization equilibrates (in this case vanishes to zero everywhere). c). The C^{zz} correlation function equilibrates, whereas the C^{xx} correlation function acquires spatial oscillations at wave-vector $\sim \frac{h_0}{\pi v_F}$ which is related to the change in the magnetization from one end of the initial domain-wall to the other. These results are in good agreement with the exact results of section II obtained from solving the fermion lattice problem. Thus bosonization is good at capturing the behavior at long distances and times, even for the nonequilibrium problem. As expected it misses some of the details of the short distance physics both in the static properties (as shown in Fig. 5), as well as during the time-evolution such as the existence of a complex internal structure in the propagating domain wall front²⁵.

In the next section we provide an explanation for the inhomogeneities observed in the transverse spin correlation function by solving the classical equations of motion for the spins.

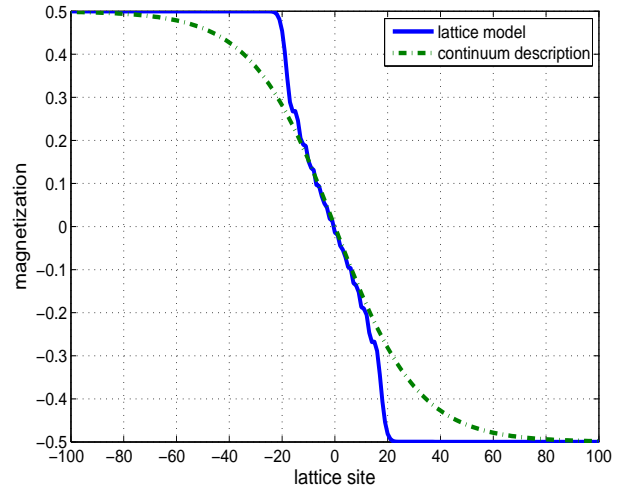


FIG. 5: Plot of the magnetization obtained from the bosonization approach with $h(x) = h_0 \tanh x/\xi$, and from the fermionic lattice model with $\alpha = 20$.

IV. MAGNETIC FIELD QUENCH IN A CLASSICAL SPIN CHAIN: FORMATION OF A TRANSVERSE SPIN-WAVE PATTERN

The Hamiltonian in Eq. 1 implies the following equations of motion for the spins

$$\frac{dS_j^z}{dt} = -J [S_j^y (S_{j+1}^x + S_{j-1}^x) - S_j^x (S_{j+1}^y + S_{j-1}^y)] \quad (79)$$

$$\frac{dS_j^x}{dt} = -JS_j^z (S_{j+1}^y + S_{j-1}^y) - h_j S_j^y \quad (80)$$

$$\frac{dS_j^y}{dt} = JS_j^z (S_{j+1}^x + S_{j-1}^x) + h_j S_j^x \quad (81)$$

We will treat the spins as classical variables, and solve the above equations for a sudden quench of a spatially inhomogeneous magnetic field, $h_j(t) = h_j \theta(-t)$. First notice that for $t \leq 0$, after performing the course-graining $S_j^a = S_{j+1}^a$, the following spin profile satisfy the equations of motion,

$$S_j^z = -\frac{h_j}{2J} \quad (82)$$

$$S_j^x = \sqrt{S^2 - (S_j^z)^2} \quad (83)$$

$$S_j^y = 0 \quad (84)$$

With the above as an initial condition, the dynamics for $t > 0$ can be easily studied numerically and we find a ballistic spreading out of the domain wall profile (see Fig. 6), and the appearance of a spin-wave pattern. The latter result, *i.e.*, the appearance of an inhomogeneous pattern at long times can be verified analytically rather easily as follows. Suppose, $h_j(t) = -h_0 \tanh \frac{x}{\xi} \theta(-t)$.

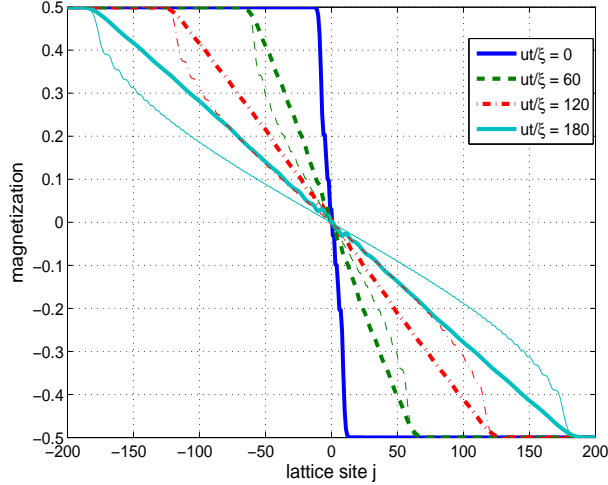


FIG. 6: Solid line: Time evolution of the magnetization from the solution of the classical Landau-Lifshitz equation assuming that $S_z(t \leq 0)$ is given by Eq. 9. Dashed lines: Time evolution from the exact solution of the quantum problem.

Then for $t > 0$, if we assume a ballistic broadening of the domain wall,

$$S_j^z(t) = \frac{h_0}{2J} \left[\tanh\left(\frac{ja - vt}{\xi}\right) + \tanh\left(\frac{ja + vt}{\xi}\right) \right] \quad (85)$$

Writing Eq. 80, 81 in terms of $S^\pm = S^x \pm iS^y$, and performing a course-graining, one obtains the following equation for $S^+(x = ja)$

$$\frac{dS^+(x, t)}{dt} = 2iJS^z(x, t)S^+(x, t) \quad (86)$$

Using Eq. 85, Eq. 86 may be easily solved to obtain

$$S^+(x, t) = S^+(x, 0) \exp \left[\frac{ih_0\xi}{2v} \left(\ln \frac{\cosh(\frac{vt+x}{\xi})}{\cosh(\frac{vt-x}{\xi})} \right) \right] \quad (87)$$

Thus for $vt \gg |x|$ we find the spin-wave pattern

$$S^+(x, t) \rightarrow S^+(x, 0)e^{ih_0x/v} \quad (88)$$

in agreement with the results of the previous sections.

Thus the appearance of the spatial inhomogeneity may be understood as follows. Right after the magnetic field is switched off, the spins in the XY plane begin to precess due to a non-zero magnetization in the z-direction. However this precession only lasts for as long as it takes the domain wall profile to flatten out to zero. Since this time is different for spins located at different spatial positions, the spins locally dephase with respect to each other and arrange themselves in a spin-wave pattern.

V. QUENCH OF A SPATIALLY VARYING MAGNETIC FIELD AND INTERACTIONS IN A XXZ CHAIN: BOSONIZATION APPROACH

A. Quench within the massless XX phase

We will now turn our attention to the case where as the magnetic field is switched off at $t = 0$, the interactions are also turned on so that the Luttinger parameter is $K = \theta(-t) + K\theta(t)$. We will first consider the case where the ground state both before and after the quench corresponds to a gapless XX phase, so that the $\cos(\beta\phi)$ term can be neglected.

1. Bogoliubov rotation

We wish to begin with a non-interacting system in an inhomogeneous magnetic field,

$$\begin{aligned} H_i &= \frac{v_F}{2\pi} \int dx \left((\nabla\phi)^2 + (\nabla\theta)^2 + \frac{2}{v_F} h(x)\nabla\phi \right) \\ &= \sum_{p \neq 0} v_F |p| a_p^\dagger a_p, \end{aligned} \quad (89)$$

and quench to zero field, while turning on interactions so that

$$\begin{aligned} H_f &= \frac{u}{2\pi} \int dx \left(\frac{1}{K} (\nabla\phi)^2 + K (\nabla\theta)^2 \right) \\ &= \sum_{p \neq 0} u |p| \eta_p^\dagger \eta_p. \end{aligned} \quad (91)$$

The η_p operators have a simple time evolution and may be related to the b_p operators by a Bogoliubov rotation^{9,10},

$$\eta_p = \cosh \beta b_p + \sinh \beta b_{-p}^\dagger, \quad (93)$$

$$\eta_p^\dagger = \cosh \beta b_p^\dagger + \sinh \beta b_{-p}. \quad (94)$$

where $e^{-2\beta} = K$. We define,

$$f(p, t) = \cos(u|p|t) - i \sin(u|p|t) \cosh(2\beta), \quad (95)$$

$$g(p, t) = i \sin(u|p|t) \sinh(2\beta). \quad (96)$$

and $\alpha_\pm \equiv f(p, t) \pm g(p, t)$. Performing the shift $b_p = a_p + \lambda_p$ as before, we write the ϕ and θ fields as $(\phi, \theta) = (\phi_\beta^a, \phi_\beta^a) + \delta(\phi_\beta, \theta_\beta)$, where

$$\begin{aligned} \phi_\beta^a(x, t) &= \frac{-i\pi}{L} \sum_{p \neq 0} \left(\frac{L|p|}{2\pi} \right)^{1/2} \frac{1}{p} e^{-\alpha|p|/2 - ipx} (\alpha_+^* a_p^\dagger \\ &+ \alpha_+ a_{-p}) \end{aligned} \quad (97)$$

$$\begin{aligned} \theta_\beta^a(x, t) &= \frac{i\pi}{L} \sum_{p \neq 0} \left(\frac{L|p|}{2\pi} \right)^{1/2} \frac{1}{|p|} e^{-\alpha|p|/2 - ipx} (\alpha_-^* a_p^\dagger \\ &+ \alpha_- a_{-p}), \end{aligned} \quad (98)$$

The $\delta(\phi, \theta)$ arise due to the spatially varying magnetic field and are given by,

$$\delta\phi_\beta(x, t) = \frac{u}{v_F} \delta\phi(x, t, \beta = 0, v_F \rightarrow u), \quad (99)$$

$$\delta\theta_\beta(x, t) = \frac{ue^{2\beta}}{v_F} \delta\theta(x, t, \beta = 0, v_F \rightarrow u), \quad (100)$$

where $\delta\phi(x, t, \beta = 0, v_F), \delta\theta(x, t, \beta = 0, v_F)$ are given in Eq. 62 and 63 respectively.

2. Magnetization after the quench

It is straightforward to show that the magnetization at a time t after the quench is

$$S_z(x, t) = -\frac{1}{\pi} \frac{\partial \delta\phi(x)}{\partial x} = \frac{1}{2\pi v_F} [h(x + ut) + h(x - ut)] \quad (101)$$

Thus even with the interaction quench, the domain wall spreads out ballistically, but with the renormalized velocity u .

3. Basic non-equilibrium correlations

To compute the correlation functions, some basic expressions we need are

$$G_{\phi\phi} = \langle [\phi_\beta^\alpha(x, t) - \phi_\beta^\alpha(x', t)]^2 \rangle \quad (102)$$

$$G_{\theta\theta} = \langle [\theta_\beta^\alpha(x, t) - \theta_\beta^\alpha(x', t)]^2 \rangle \quad (103)$$

Note that $G_{\theta\theta}$ is related to $G_{\phi\phi}$, $K \rightarrow \frac{1}{K}$ the computation of which is identical to that already presented in^{9,10}. For completeness we present the results below,

$$G_{\phi\phi} = \int_0^\infty \frac{dp}{p} [\cos^2(utp) + e^{-4\beta} \sin^2(utp)] \times (1 - \cos[p(x - x')]) e^{-\alpha p} \quad (104)$$

which eventually gives

$$G_{\phi\phi} = G_{\phi\phi}^{(0)} + \left(\frac{K^2 - 1}{8} \right) \times \log \left[\frac{[\alpha^2 + (2ut)^2][\alpha^2 + x^2]^2}{\alpha^4[\alpha^2 + (2ut + x)^2][\alpha^2 + (x - 2ut)^2]} \right] \quad (105)$$

$$G_{\theta\theta} = G_{\theta\theta}^{(0)} + \left(\frac{K^{-2} - 1}{8} \right) \times \log \left[\frac{[\alpha^2 + (2ut)^2][\alpha^2 + x^2]^2}{\alpha^4[\alpha^2 + (2ut + x)^2][\alpha^2 + (x - 2ut)^2]} \right]. \quad (106)$$

where $G_{\phi\phi}^{(0)} = \frac{K}{2} \log \left[\frac{x^2 + \alpha^2}{\alpha^2} \right], G_{\theta\theta}^{(0)} = \frac{1}{2K} \log \left[\frac{x^2 + \alpha^2}{\alpha^2} \right]$.

4. Spin correlations after the quench

Taking the $2ut \gg x$ limit, we can easily obtain the correlator asymptotics. The memory of the initial domain wall profile appears as oscillatory pre-factors of the form $\exp[2i(\delta\phi(x + n) - \delta\phi(x))]$ and terms such as $\nabla\delta\phi(x + n)\nabla\delta\phi(x)$. For the specific case of $h(x) = h_0 \tanh(x/\xi)$ we find,

$$\langle \hat{S}^z(x + n) \hat{S}^z(x) \rangle = f(x + n, t) f(x, t) + \frac{C'_1}{n^2} + \frac{C'_2(-1)^n}{n^{K^2+1}} \quad (107)$$

$$\langle \hat{S}^+(x + n) \hat{S}^-(x) \rangle = \frac{C'_3 \exp[ih_0 n/v_F K]}{n^{1+K^2+\frac{1+K^2}{4}}} + \frac{C'_4(-1)^n \exp[ih_0 n/v_F K]}{n^{\frac{1+K^2}{4}}} \quad (108)$$

where

$$f(x, t) = \frac{1}{2v_F} (h(x + ut) + h(x - ut)) \quad (109)$$

The case of the pure interaction quench ($h_0 = 0$) was studied in^{9,10} where the above anomalous power-laws corresponding to an algebraic decay which is faster than in the equilibrium case (since $K^2 + 1 \geq 2K$ for all real K) were obtained. Here we find that the effect of an initial domain wall profile is to superimpose spatial oscillations at wavelength $\sim v_F K/h_0$ onto this decay.

5. Generalized Gibb's Ensemble ?

Rigol *et al* have made the interesting proposal that the long-time properties of out of equilibrium integrable systems may be captured by a generalized Gibb's ensemble that enforces the constraints imposed by the integrals of motion²⁶. This approach has been applied with success by Iucci and Cazalilla^{9,10} who studied homogeneous interaction quenches in models similar to those studied in this paper. We on the other hand find that for inhomogeneous quantum quenches, the Gibb's ensemble argument cannot capture the spatial inhomogeneities at long times after the quench. In this section we review the Gibb's ensemble argument and show why this does not work for our case.

Consider a quantum quench of the form $H = H_i\theta(-t) + H_f\theta(t)$, so that for $t \leq 0$ the system is in the ground state of H_i , whereas at $t > 0$, the wave-function begins to evolve according to H_f . Let us further assume that both H_i and H_f can be diagonalized

$$H_i = \sum_p \epsilon_p^a a_p^\dagger a_p \quad (110)$$

$$H_f = \sum_p \epsilon_p^b b_p^\dagger b_p \quad (111)$$

and that the two Hilbert spaces may be related to each other via a canonical transformation. For the case of bosons a general canonical transformation is of the form,

$$b_p = \cosh \Theta_p a_p + \sinh \Theta_p a_{-p}^\dagger + \lambda_p \quad (112)$$

where λ_p and the rotation angle Θ_p are constants.

The essential idea behind predicting the long-time behavior is that an integrable model such as H_f has a conserved quantity for every degree of freedom. For the example given above, the conserved quantity is trivially given by $I_p = b_p^\dagger b_p$. Thus during the time-evolution $\langle b_p^\dagger b_p \rangle$ should be conserved. Since the initial state is the ground state of H_i for which $\langle a_p^\dagger a_p \rangle = 0$ for $p \neq 0$, it follows that the Gibbs' ensemble should be characterized by the distribution function

$$\langle b_p^\dagger b_p \rangle = |\lambda_p|^2 + \sinh^2 \Theta_p. \quad (113)$$

For the particular models studied here, we find the initial spatial inhomogeneity is captured by the linear shift λ_p (given by Eq. 56), while the angle Θ_p captures the homogeneous changes in the interaction parameter. Since $|\lambda_p|^2$ vanishes in the thermodynamic limit, any effect of the initial spatial inhomogeneity is lost. Thus while the Gibb's ensemble captures the effect of the rotation, and therefore correctly predicts the new power law exponents of⁹, it misses the spin-wave pattern at long times.

B. Magnetic field and Interaction quench into the Ising phase: Semiclassical treatment

In this section we will study the effect of quenching the external magnetic field and the interactions into the massive Ising phase where the $\cos \phi$ term is strongly relevant. In order to study the time evolution, we will employ a semi-classical approximation which corresponds to replacing $\cos \phi \sim 1 - \frac{\phi^2}{2}$. Thus for this case the initial wave-function is the ground state of

$$\begin{aligned} H_i &= \frac{v_F}{2\pi} \int dx \left[(\nabla \phi)^2 + (\nabla \theta)^2 + \frac{2}{v_F} h(x) \nabla \phi \right] \quad (114) \\ &= \sum_p v_F |p| a_p^\dagger a_p \quad (115) \end{aligned}$$

while for $t > 0$ the wave-function evolves according to

$$H_f = \frac{u}{2\pi} \int dx \left[(\nabla \tilde{\phi})^2 + (\nabla \tilde{\theta})^2 + \frac{m^2}{u^2} \tilde{\phi}^2 \right] \quad (116)$$

$$= \sum_p \omega_p \eta_p^\dagger \eta_p \quad (117)$$

where $\tilde{\phi} = \frac{\phi}{\sqrt{K}}$, $\tilde{\theta} = \sqrt{K} \theta$ and $\omega_p = \sqrt{p^2 u^2 + m^2}$.

The calculations mirror that of the previous section. Writing $\phi = \phi^\alpha + \delta\phi$, $\theta = \theta^\alpha + \delta\theta$, we find for a time t

after the quench

$$\begin{aligned} \phi^a(x, t) &= -\frac{i\pi}{L} \sum_{p \neq 0} \left(\frac{L|p|}{2\pi} \right)^{1/2} \\ &\times \frac{1}{p} e^{-\alpha|p|/2 - ipx} \left[a_p^\dagger \left(\cos(\omega_p t) + iK \frac{u|p|}{\omega_p} \sin(\omega_p t) \right) \right. \\ &\left. + a_{-p} \left(\cos(\omega_p t) - iK \frac{u|p|}{\omega_p} \sin(\omega_p t) \right) \right], \quad (118) \end{aligned}$$

$$\begin{aligned} \theta^a(x, t) &= \frac{i\pi}{L} \sum_{p \neq 0} \left(\frac{L|p|}{2\pi} \right)^{1/2} \\ &\times \frac{1}{|p|} e^{-\alpha|p|/2 - ipx} \left[a_p^\dagger \left(\cos(\omega_p t) + i \frac{\omega_p}{Ku|p|} \sin(\omega_p t) \right) \right. \\ &\left. - a_{-p} \left(\cos(\omega_p t) - i \frac{\omega_p}{Ku|p|} \sin(\omega_p t) \right) \right] \quad (119) \end{aligned}$$

and

$$\begin{aligned} \delta\phi(x, t) &= \frac{i}{\pi v_F} \int_0^\infty \frac{dp}{p} \cos[\omega_p t] \cos[px] h_p, \quad (120) \\ \delta\theta(x, t) &= \frac{-i}{\pi K v_F} \int_0^\infty \frac{dp}{p} \sin[\omega_p t] \sin[px] \left(\frac{\omega_p}{u|p|} \right) h_p \quad (121) \end{aligned}$$

1. Magnetization after the quench

The magnetization at a time t after the quench is given by $\langle S^z(x, t) \rangle = -\frac{1}{\pi} \partial_x \phi(x, t) + \frac{(-1)^x}{\pi\alpha} \langle \cos(2\phi(x, t)) \rangle$. Due to the presence of infra-red divergences, we find that for all times after the quench,

$$\langle e^{-2i\phi(x, t)} \rangle \sim 0 \quad (122)$$

so that Ising order never develops. This is consistent with the results of¹⁰ and may be an artifact of the semi-classical approximation. In section VI we will compare this result with a mean-field treatment for the order-parameter dynamics.

Thus, within the validity of the semiclassical approximation we find the following time evolution for the initial domain wall profile,

$$\begin{aligned} \langle S^z(x, t) \rangle &= -\frac{1}{\pi} \partial_x (\delta\phi(x, t)) \\ &= \frac{h_0}{\pi v_F} \int_0^\infty dz \cos \left(\frac{ut}{\xi} \sqrt{z^2 + \left(\frac{m\xi}{u} \right)^2} \right) \\ &\times \frac{\sin \left(\frac{x}{\xi} z \right)}{\sinh \left(\frac{\pi z}{2} \right)} \quad (123) \end{aligned}$$

The above is plotted in Fig. 7 for several different masses. The domain wall profile shows a more complex time evolution than for the quench in the gapless phase where a

simple ballistic broadening of the domain wall occurs. In the Ising phase instead we find oscillations of the local magnetization at the frequency of the mass. In addition the domain wall spreads out less and less as the mass increases, a result which is in agreement with a t-DMRG study of the XXZ chain⁷.

We also find that the magnetization eventually equilibrates at long times. Fig. 8 shows the time evolution for the magnetization for a given point in position space. For long times Eq. 123 may be evaluated in a stationary phase approximation which gives,

$$\langle S^z(x, t) \rangle \simeq \frac{2h_0 x}{\pi v_F} \sqrt{\frac{2m}{\pi u^2 t}} \cos\left(mt + \frac{\pi}{4}\right) \quad (124)$$

showing that the magnetization decays locally as a power-law.

2. Correlation functions after the quench

Here we give results for some typical spin correlation functions. Again, due to the presence of infra-red divergences, the transverse-spin correlation function is found to vanish at all times after the quench,

$$\langle e^{i\theta(x,t)} e^{-i\theta(0,t)} \rangle \sim 0 \quad (125)$$

On the other hand the $z-z$ correlation function is found to be

$$\langle e^{2i\phi(x,t)} e^{-2i\phi(0,t)} \rangle = e^{2i(\delta\phi(x,t) - \delta\phi(x,0))} A'(\alpha) \left(\frac{1}{x}\right) \quad (126)$$

For a purely interaction quench ($\delta\phi = 0$) we find a power law decay in the Ising phase with an exponent which is half of that in the initial gapless phase, a result which was also found by¹⁰. The initial domain profile superimposes the additional structure

$$e^{2i(\delta\phi(x,t) - \delta\phi(y,0))} \xrightarrow{mt \gg 1} e^{2i \left[\frac{h_0(x^2 - y^2)}{v_F} \sqrt{\frac{2m}{\pi u^2 t}} \cos\left(mt + \frac{\pi}{4}\right) \right]} \quad (127)$$

Thus at long times, the spatial oscillations due to the initial domain-wall eventually decay to zero.

VI. EFFECT OF QUENCHING A MAGNETIC FIELD AND INTERACTIONS: MEAN-FIELD TREATMENT

In this section we will use a mean-field argument to explore whether after quenching both a magnetic field as well as interactions, local anti-ferromagnetic (AF) Ising order can develop. Thus our initial wave-function corresponds to the ground state of the following Hamiltonian

$$H_i = J \sum_j \left[S_j^x S_{j+1}^x + S_j^y S_{j+1}^y + \frac{h_j}{J} S_j^z \right] \quad (128)$$

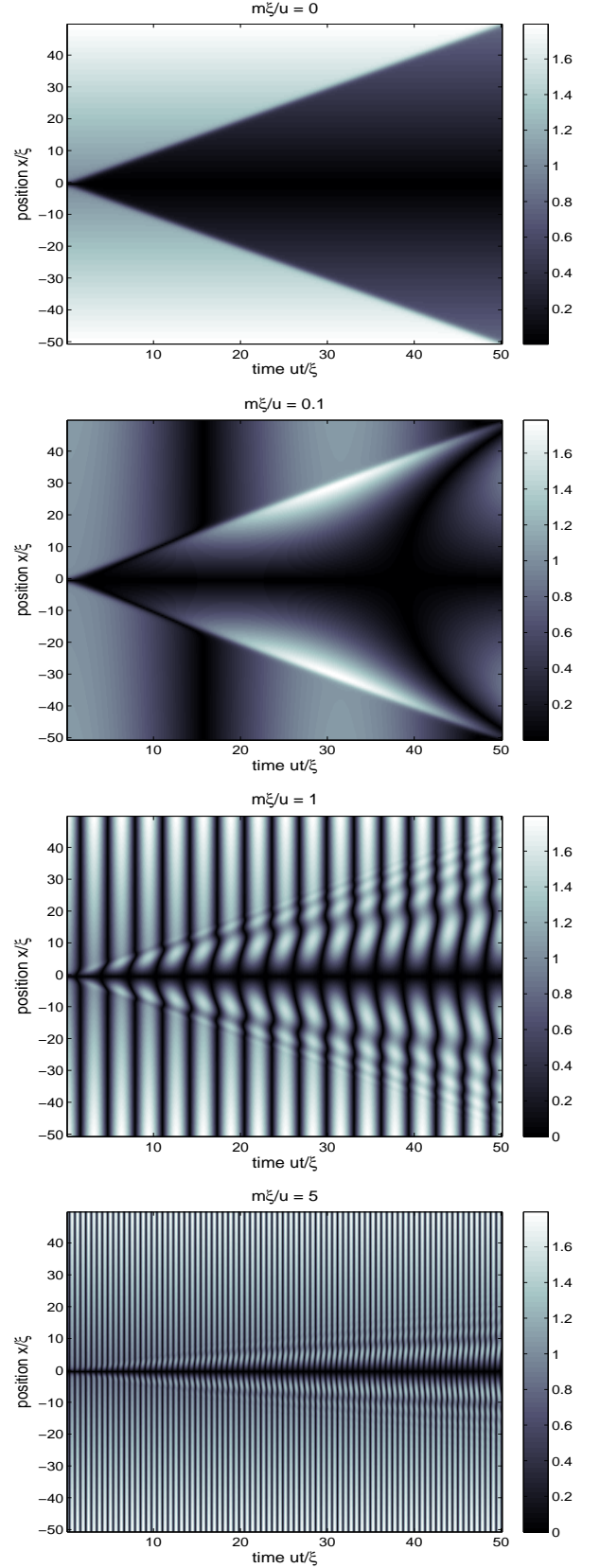


FIG. 7: Contour plot for $|S_z|$ after a “semi-classical” quench for several different masses.

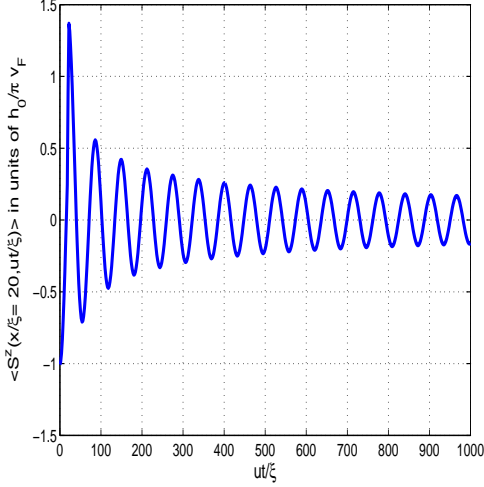


FIG. 8: The magnetization decays as $t^{-1/2}$ with oscillations of period $\sim m^{-1}$. Here, $m\xi/u = 0.1$.

with $J > 0$, and we will assume $h_j = \mathcal{F}ja$. While, as a result of the quench the wave-function evolves in time due to

$$H_f = J \sum_j (S_j^x S_{j+1}^x + S_j^y S_{j+1}^y) + J^z \sum_j S_j^z S_{j+1}^z \quad (129)$$

Performing a Jordan-Wigner transformation followed by the change of variables $c_i \rightarrow (-1)^i c_i$, H_i becomes identical to the Hamiltonian (Eq. 2) already studied in section II A, whereas the Hamiltonian after the quench is,

$$H_f = -\frac{J}{2} \sum_i (c_i^\dagger c_{i+1} + h.c.) + J^z \sum_i \left(c_i^\dagger c_i - \frac{1}{2} \right) \left(c_{i+1}^\dagger c_{i+1} - \frac{1}{2} \right) \quad (130)$$

Thus the initial state which is the ground state of H_i (given by Eq. 7) evolves in time according to Eq. 130. In what follows we will study this time evolution using a mean-field approximation.

Defining the AF order-parameter at a time t , $\Delta_0(t)$ as $\langle c_i^\dagger(t) c_i(t) \rangle = \frac{1}{2} + (-1)^i \Delta_0(t)$, Eq. 130 within a mean-field approximation becomes

$$H_f^{mf} = \sum_{|k| < \pi/2} \epsilon_k (c_k^\dagger c_k - c_{k+\pi}^\dagger c_{k+\pi}) - 2J^z \Delta_0(t) \sum_{|k| < \pi/2} (c_k^\dagger c_{k+\pi} + c_{k+\pi}^\dagger c_k) \quad (131)$$

where $\epsilon_k = -J \cos ka$, and $\Delta_0(t)$ is determined from the self-consistency condition

$$\Delta_0(t) = \frac{1}{N} \langle \Psi | e^{iH_f^{mf} t} \sum_i (-1)^i c_i^\dagger c_i e^{-iH_f^{mf} t} | \Psi \rangle \quad (132)$$

where N is the total number of sites.

In terms of the amplitudes $\tilde{c}_{k\pm}$ of being in the adiabatic eigenstates of H_f^{mf} , the self-consistency condition becomes

$$\begin{aligned} \Delta_0(t) = & \frac{1}{2N} \sum_{|k| < \pi/2} [\sin 2\theta_k(t) (|\tilde{c}_{k+}(t)|^2 - |\tilde{c}_{k-}(t)|^2) \\ & - \cos 2\theta_k(t) (\tilde{c}_{k+}^*(t) \tilde{c}_{k-}(t) + \tilde{c}_{k-}^*(t) \tilde{c}_{k+}(t)) \times \\ & \cos\left(\int_0^t dx (E_{k+}(x) - E_{k-}(x))\right) \\ & - i \cos 2\theta_k(t) (\tilde{c}_{k+}^*(t) \tilde{c}_{k-}(t) - \tilde{c}_{k-}^*(t) \tilde{c}_{k+}(t)) \times \\ & \sin\left(\int_0^t dx (E_{k+}(x) - E_{k-}(x))\right)] \quad (133) \end{aligned}$$

where

$$E_{k\pm}(t) = \pm \sqrt{\epsilon_k^2 + 4J_z^2 \Delta_0^2(t)} \quad (134)$$

$$\tan 2\theta_k(t) = -\frac{2J_z \Delta_0(t)}{\epsilon_k} \quad (135)$$

and the coefficients $\tilde{c}_{k\pm}$ satisfy the equations of motion,

$$\frac{d\tilde{c}_{k\pm}(t)}{dt} = \tilde{c}_{k\mp}(t) \left[\frac{\pm \epsilon_k J_z \frac{d\Delta_0}{dt}}{\epsilon_k^2 + 4J_z^2 \Delta_0^2} \right] e^{\pm i \int_0^t dx (E_{k+}(x) - E_{k-}(x))} \quad (136)$$

In an adiabatic approximation $\frac{\dot{\Delta}_0}{\Delta_0} \ll 1$, we can approximate $\tilde{c}_{k\pm}$ by its value at $t = 0$. In this case Eq. 133 becomes

$$\begin{aligned} \Delta_0 \simeq & \frac{1}{2N} \sum_{|k| < \pi/2} [\sin 2\theta_k(t) (\sin 2\theta_k(t) I_k^x + \cos 2\theta_k(t) I_k^z) \\ & - \cos 2\theta_k(t) (\sin 2\theta_k(t) I_k^z - \cos 2\theta_k(t) I_k^x) \times \\ & \cos\left(\int_0^t dx (E_{k+}(x) - E_{k-}(x))\right) \\ & - i \cos 2\theta_k(t) I_k^y \sin\left(\int_0^t dx (E_{k+}(x) - E_{k-}(x))\right)] \quad (137) \end{aligned}$$

where $I_k^{x,y,z}$ denote the following expectation values in the initial state before the quench,

$$I_k^x = \langle \Psi | c_k^\dagger c_{k+\pi} + c_{k+\pi}^\dagger c_k | \Psi \rangle \quad (138)$$

$$I_k^z = \langle \Psi | c_k^\dagger c_k - c_{k+\pi}^\dagger c_{k+\pi} | \Psi \rangle \quad (139)$$

$$I_k^y = \langle \Psi | c_{k+\pi}^\dagger c_k - c_k^\dagger c_{k+\pi} | \Psi \rangle \quad (140)$$

Since in the initial domain wall state, $I_k^{x,y,z} \sim 0$, this implies that $\Delta_0(t) = 0$, and hence anti-ferromagnetic order does not develop within a mean-field and adiabatic approximation. This result can also be understood from the fact that the initial state is a highly excited state of the anti-ferromagnetic model as it corresponds to introducing a domain wall in the staggered magnetization at almost every site⁷.

The above conclusion also holds if we relax the adiabatic approximation. To see this note that at every k , the mean-field Hamiltonian Eq. 131 corresponds to a pseudo-spin 1/2 $\vec{\tau}_k$ where²⁷ $\tau_k^z = c_k^\dagger c_k - c_{k+\pi}^\dagger c_{k+\pi}$, $\tau_k^x = c_k^\dagger c_{k+\pi} + c_{k+\pi}^\dagger c_k$ and $\tau_k^y = i(c_{k+\pi}^\dagger c_k - c_k^\dagger c_{k+\pi})$. This pseudo-spin is subjected to a magnetic field that has to be determined self-consistently at each time t where for $t = 0$ $\langle \tau_k^{x,z}(0) \rangle = I_k^{x,z}$, $\langle \tau_k^y(0) \rangle = iI_k^y$. Since for the initial domain wall state $\langle \vec{\tau}(0) \rangle = 0$, it implies $\frac{d^n \langle \tau_k^x \rangle}{dt^n}(t = 0) = 0$ to all orders in n , so that anti-ferromagnetic order ($\propto \sum_k \langle \tau_k^x \rangle$) will not develop.

VII. CONCLUSIONS

In summary we have studied quenched dynamics in a XXZ chain starting from an initial inhomogeneous state where the spins are arranged in a domain wall profile. The dynamics of the domain wall is found to be qualitatively different within the gapless XX phase and the gapped Ising phase. In the former the domain wall broadens ballistically, while in the latter the domain wall spreads out less and less the deeper one is in the Ising phase. The magnetization is locally found to oscillate, and eventually decays as a power-law. Although the results in the Ising phase were obtained within a semiclassical treatment, they are in qualitative agreement with t-DMRG simulations of the XXZ chain^{7,8}.

We have also presented results for the time-evolution of two-point correlation functions. For quenches within the gapless XX phase we find that while the longitudinal spin correlation function (C^{zz}) reaches the ground state value, the transverse spin correlation function (C^{xx}) do not equilibrate, but have a spin wave pattern superimposed on them. This is found to arise due to dephasing of transverse spin components as the domain wall broadens. We also find that a Gibb's ensemble argument is not adequate in capturing this spatially inhomogeneous pattern.

For quenches into the gapped Ising phase, all inhomogeneities both in the single particle and two-particle expectation values are found to eventually decay away. This may be an artifact of the semiclassical approximation which neglects soliton creation.¹⁰ We would also like to point out a recent preprint²⁸ that studies time-evolution of an initial domain wall in the gapped Ising phase using Algebraic Bethe Ansatz. The authors study the Loschmidt echo and find a lack of thermalization.

Finally we perform a mean-field treatment for the time-evolution of the anti-ferromagnetic gap and find that for an initial state corresponding to a domain wall

profile, anti-ferromagnetic order never develops. This should be expected on the grounds that the initial domain wall profile corresponds to a highly excited state of the anti-ferromagnetic Ising model.

Acknowledgments

The authors are particularly indebted to Eugene Demler and Ulrich Schollwöck for helpful discussions. This work was supported by NSF-DMR (Contract No. 0705584).

Appendix A: Diagonalization of the XX-model

The Hamiltonian for the XX model is

$$H_{xx} = -J \sum_j [S_j^x S_{j+1}^x + S_j^y S_{j+1}^y]. \quad (\text{A1})$$

The Hamiltonian may be diagonalized by the Jordan-Wigner fermionic operators c_j and c_j^\dagger defined in terms of the spin raising and lowering operators $S_j^\pm = S_j^x \pm iS_j^y$ as follows,

$$S_j^- = \exp \left[-i\pi \sum_{n=-N/2+1}^{j-1} c_n^\dagger c_n \right] c_j, \quad (\text{A2})$$

$$S_j^+ = \exp \left[i\pi \sum_{n=-N/2+1}^{j-1} c_n^\dagger c_n \right] c_j^\dagger, \quad (\text{A3})$$

The Hamiltonian is diagonal in momentum space $c_j = \frac{1}{\sqrt{N}} \sum_k c_k e^{ikj}$ where,

$$H_{xx} = \sum_k \epsilon_k c_k^\dagger c_k \quad (\text{A4})$$

$$\epsilon_k = -J \cos k. \quad (\text{A5})$$

Thus the operators c_k , have the trivial time-evolution $c_k(t) = c_k(0)e^{-i\epsilon_k t}$. In terms of the η_m quasi-particles that diagonalize the Wannier-Stark problem (Eq. 2), the transformation given by Eqns. (5, 6) yields

$$c_j(t) = \frac{1}{N} \sum_{k,m} e^{ik(j-m) - i\alpha \sin k} e^{-i\epsilon_k t} \eta_m \quad (\text{A6})$$

$$c_j^\dagger(t) = \frac{1}{N} \sum_{k,m} e^{-ik(j-m) + i\alpha \sin k} e^{i\epsilon_k t} \eta_m^\dagger \quad (\text{A7})$$

¹ I. Bloch, J. Dalibard and W. Zwerger, *Rev. Mod. Phys.* **80**, 885 (2008).

² T. Kinoshita, T. Wenger, and D. S. Weiss, *Nature*, **440** 900 (2006).

³ T. Giamarchi, *Quantum Physics in One Dimension*, (Oxford University Press, Oxford, 2004).

⁴ K. Sengupta, S. Powell and S. Sachdev, *Phys. Rev. A* **69**, 053616 (2004).

- ⁵ P. Barmettler, M. Punk, V. Gritsev, E. Demler and E. Altman, *Phys. Rev. Lett.* **102**, 130603 (2009).
- ⁶ D. M. Weld, P. Medley, H. Miyake, D. Hucul, D. E. Pritchard, and W. Ketterle *Phys. Rev. Lett.* **103**, 245301 (2009).
- ⁷ D. Gobert, C. Kollath, U. Schollwöck, and G. Schütz, *Phys. Rev. E* **71**, 036102 (2005).
- ⁸ S. Langer, F. Heidrich-Meisner, J. Gemmer, I. P. McCulloch, and U. Schollwöck, *Phys. Rev. B* **79**, 214409 (2009).
- ⁹ M. A. Cazalilla, *Phys. Rev. Lett.* **97**, 156403 (2006).
- ¹⁰ A. Iucci and M. A. Cazalilla, arXiv:0903.1205v2.
- ¹¹ E. Lieb, T. Schultz, and D. Mattis, *Ann. Phys. (N.Y.)* **16**, 407 (1961).
- ¹² E. Barouch, B. McCoy, and M. Dresden, *Phys. Rev. A* **2**, 1075-1091 (1970).
- ¹³ E. Barouch and B. McCoy, *Phys. Rev. A* **2**, 786-804 (1971).
- ¹⁴ E. Barouch and B. McCoy, *Phys. Rev. A* **3**, 2137-2140 (1971).
- ¹⁵ E. R. Smith, *Physica* **53**, 289 (1971).
- ¹⁶ K. M. Case and C. W. Lau, *J. Math. Phys.*, **14**, 720 (1973).
- ¹⁷ T. Hartmann, F. Keck, H. J. Korsch, and S. Mossmann, *New J. Phys.* **6**, 2 (2004).
- ¹⁸ *Handbook of Mathematical Functions*, edited by M. Abramowitz and I. A. Stegun (Dover: New York, 1965).
- ¹⁹ T. Antal, Z. Rácz, A. Rakos, G. M. Schutz, *Phys. Rev. E* **59**, 4912 (1999).
- ²⁰ Note that in the limit of a large number of sites, the result is insensitive to whether the $m = 0$ mode is included in the sum or not.
- ²¹ A. A. Ovchinnikov, *Phys. Lett. A*, **377**, 357 (2007).
- ²² P. Calabrese and J. Cardy, *Phys. Rev Lett.* **96** 136801 (2006).
- ²³ S. Sotiriadis and J. Cardy, *J. Stat. Phys.* **P11003** (2008).
- ²⁴ P. Calabrese, C. Hagendorf and P. Le Doussal, *J. Stat. Mech.* P07013 (2008).
- ²⁵ V. Hunyadi, Z. Rácz, and L. Sasvári, *Phys. Rev. E* **69**, 066103 (2004).
- ²⁶ M. Rigol, V. Dunjko, V. Yurovsky, and M. Olshanii, *Phys. Rev. Lett.* **98**, 050405 (2007).
- ²⁷ Peter Barmettler, Matthias Punk, Vladimir Gritsev, Eugene Demler, Ehud Altman, arXiv.0911.1927.
- ²⁸ J. Mossel and J. S. Caux, arXiv:1002.3988.